

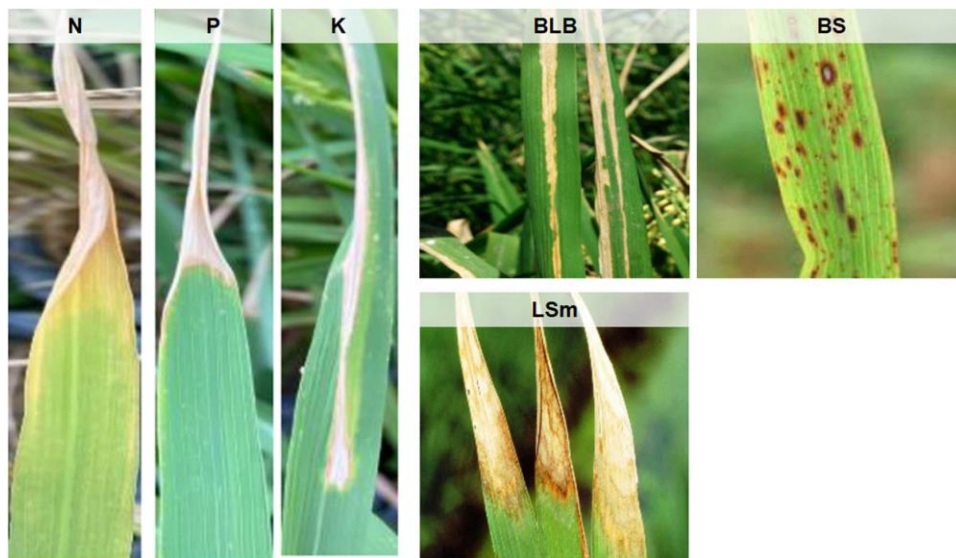
Rice Leaf Disease Analyzer + Tensorflow.js Web App

Introduction:

Rice is a staple food for a significant portion of the world's population. However, rice cultivation faces various challenges, including the susceptibility of rice plants to diseases. Timely detection and classification of these diseases are crucial for effective crop management and ensuring food security. In this project, we aim to leverage deep learning techniques to develop a model that can classify three common types of rice leaf diseases: leaf smut, brown spot, and bacterial leaf blight.

The world's population is growing day by day and will tend to increase at higher rates in the near future. The world's population has increased from 2.5 to 7.7 billion between 1950 and 2019. According to the 2019 UN report, it is predicted that the world's population would increase by 10, 26, and 42% in the periods of 2019–2030, 2019–2050, and 2019–2100, respectively. The growing population will lead to higher food consumption which in turn will increase food demand and require supply. Asia, the world's largest continent, relies heavily on rice as its staple food. Between 1961 and 2019, the world's rice production increased from 215 to 755 million tons. Global rice yield increased from 1.86 to 4.66 tonnes per hectare between 1961 and 2019. As the population has grown, so has rice production and its yield. In this manner, the rate of growth in rice yield and production must be sustained over the subsequent decades so that poverty, hunger, undernourishment, food security, etc., do not reach the critical point of failure. However, disease and nutrient deficiency disorders in rice plants act as hindrances to rice growth and yield. Numerous catastrophic diseases that affect rice plants are caused by fungi, bacteria, viruses, and lack of nutrients.

Some of the common diseases and nutrient deficiencies in rice plants are shown in [Figure 1](#).



Bacterial leaf blight (BLB) disease alone can cause up to 50% yield losses worldwide. Rice yields can also be significantly impacted by some diseases like brown spot (BS) and leaf smut (LSm). One of the most common diseases affecting rice is BS, caused by *Drechsleraoryzae*. BS lesions are often curved, brown in color, and surrounded by a yellow rim.

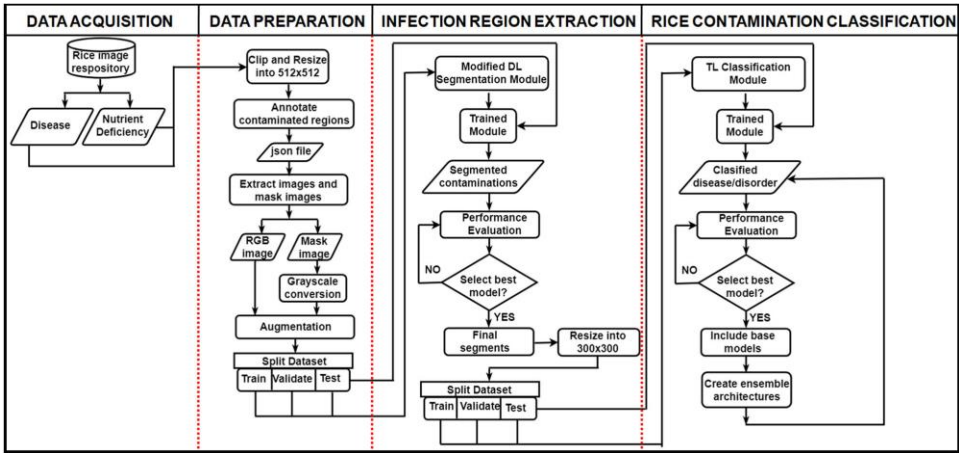
The dataset at our disposal is relatively small, consisting of only 120 images. Despite this limitation, we will employ advanced techniques to enhance our model's ability to generalize and classify unseen data accurately. The use of TensorFlow 2.0 Keras, image augmentation, and a pre-trained MobileNet model is anticipated to yield a validation accuracy score exceeding 90%.

Objective:

The goal of this project is to develop a robust model for classifying three types of rice leaf diseases - leaf smut, brown spot, and bacterial leaf blight. Despite having a limited dataset of 120 images, the use of TensorFlow 2.0 Keras, image augmentation, and a pre-trained MobileNet model will be leveraged to achieve a validation accuracy score exceeding 90%. The trained model will be deployed in a Tensorflow.js web app for online accessibility.

Methodology:

The datasets used in this study were retrieved from the Kaggle repository and UCI ML repository. The images of the input rice disease and deficiency disorders were resized and enhanced. In order to label the infected areas of the images, ground truth masks were created. After creating annotations and extracting masks of the rice leaf images, a dataset was created in the ratio of 70:30 for performing the segmentation of rice diseases. Then DL segmentation architectures were applied to this newly created dataset. The segmentation method was assessed using the following metrics: dice loss, dice coefficient, accuracy, precision, and recall.



2.1 Data preparation

2.1.1 Image acquisition

We selected two datasets that were sizable enough to offer useful information but not so large that it becomes difficult to annotate contaminated areas. The datasets include the relevant nutrient deficiencies

like N, P, and K as well as rice diseases, including BLB, BS, and LSm. Moreover, we were looking for a dataset that could be easily accessed, either through a public repository or by directly contacting the owner of the data. Therefore, the Kaggle and UCI ML datasets were chosen.

As far as law or ethics are concerned, the selected datasets may be used for research purposes without restriction. The acquired dataset contains 120 diseased rice leaf images, which include BLB, BS, and LSm varieties. The images' resolutions vary from 301×71 to $3,081 \times 897$ pixels. The images were taken in a field in the Shertha village of Gujarat, India, using a 12.3 megapixel NIKON D90 digital SLR camera during the winter season. This dataset has 120 images in the .jpeg format, including 40 images of each disease [41].

The Kaggle rice nutrient deficiency images consist of three types of deficiencies, namely nitrogen (N), phosphorous (P), and potassium (K). There are 440, 333, and 383 images in each of these classes. All the images are of varying resolutions [8]. A snapshot of the image dataset of rice diseases and deficiency disorders used in this study is shown in [Figure 4](#).

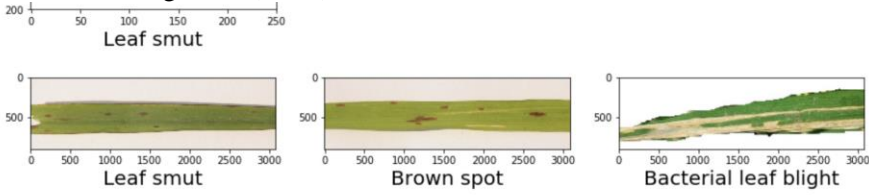


2.1.2 Image pre-processing and rice disease/deficiency disorder annotation

In order to extract multiple disease zones from a single image of a rice leaf, the images of the dataset were clipped. They were then scaled down to 512×512 pixels in resolution. After clipping and resizing, a total of 255 rice disease images were obtained. Similarly, 1,156 rice deficiency disorder images were obtained. The clipping and resizing approach used in this study is shown in Algorithm 1. No ground truth segmentation masks were present in the rice datasets. In order to evaluate the task of segmentation, the positions and categories of infected patches in the rice images were labeled using the VIA annotation tool.

Algorithm 1: Algorithm to obtain resized clipped images

Input: fl = path_to_dataset

Output: resized_image
For all_images in f1 do
box = clipping_size
image_crop = file_i.crop(box)
resized_image = image_crop.resize((512,512))
resized_image.save(file_i)


The ground truth (mask) images were then obtained from the labeled json file as shown in [Figure 5](#).

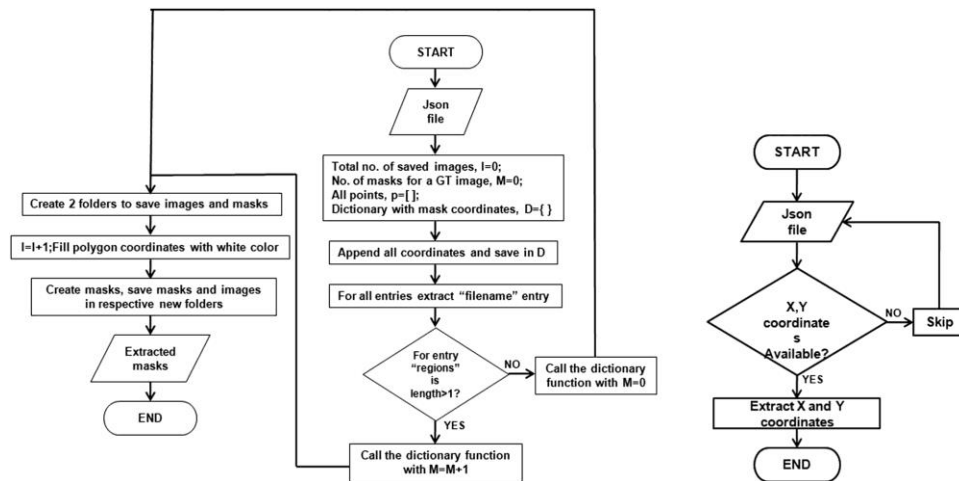


Figure 5

These extracted masks were then subjected to grayscale conversion. To increase the data samples, augmentation techniques like rotation, flip, shear, shift, and zoom were applied to the training and validation images and their corresponding masks. The augmentation parameters are given in [Table 1](#).

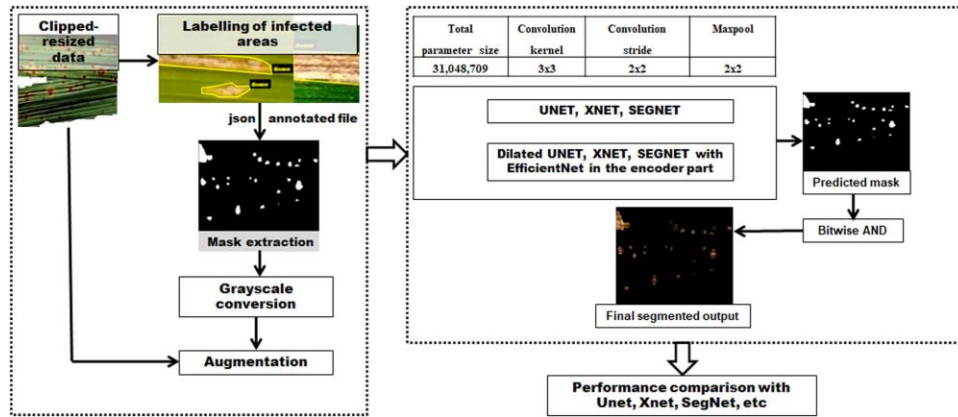
Table 1

Augmentation techniques applied in the current study

Augmentation techniques	Range/mode
Rotation	0.2
Width shift	0.05
Height shift	0.05
Shear	0.05
Zoom	[0.5, 1]
Horizontal flip	Random
Fill	Nearest newly created pixels

2.2 Rice-infected region extraction

The first module of DeepBatch framework for extracting infected regions from rice images is illustrated in [Figure 6](#). The rice disease and deficiency disorder images were processed separately. These images were divided into training-validation and testing sets in the ratio 70:30, and they were manually labeled to extract the infected regions. The labeled file provided the mask images, which were then converted into grayscale. Augmentation on RGB images and their corresponding grayscale masks resulted in more than 30,000 images and masks, for both datasets. These images were then passed through the DL segmentation models of DeepBatch.



3.1 Results of module 1 of DeepBatch

The DL segmentation framework using the modified versions of U-Net, XNet, and SegNet was used to extract infected regions in 255 rice leaf disease images and 1,156 rice deficiency disorder images. Considering the results of extracting regions infected with rice diseases, it was observed that the optimal loss value of the modified UNet segmentation changed from 0.8 to 0.22 after 50 epochs. Similarly, the optimal loss value of the modified SegNet segmentation changed from 0.86 to 0.26.

From [Table 3](#), it was observed that Dilated U-EfficientNet performed better than the rest in terms of dice loss, dice coefficient, and recall. Both UNet and dilated Seg-EfficientNet had validation losses of 0.8 after 50 epochs, which were determined to be worse than those of the other models. So, in order to conduct further comparisons, these segmentation models were ignored.

Table 3

Quantitative evaluation for extracting diseased regions in the rice leaf (module 1)

Models	Dice loss	Dice coefficient	Precision	Recall	Accuracy
UNet	0.8584	0.1416	0.7587	0.8947	0.9828
XNet	0.2267	0.7733	0.8723	0.7358	0.9840
SegNet	0.3588	0.6412	0.5364	0.8691	0.9600

Modified SegNet	0.8636	0.1364	0.0769	0.7905	0.5801
Modified XNet	0.2241	0.7759	0.8600	0.7564	0.9846
Modified UNet	0.2234	0.7766	0.8876	0.7112	0.9836

In the remaining models, a pattern of validation loss across 50 epochs was seen. [Figure 10](#) shows the loss function curves while extracting rice disease regions using DL segmentation models. It was found that although the validation loss for XNet, Dilated X-EfficientNet, and Dilated U-EfficientNet after 50 epochs was found to be 0.2, frequent fluctuations were seen in the cases of XNet and Dilated X-EfficientNet. As a result, Dilated U-EfficientNet and SegNet-EfficientNet, with a precision of 88.76 and 88.65%, respectively, were identified as the best models to obtain segmented regions of rice diseases.

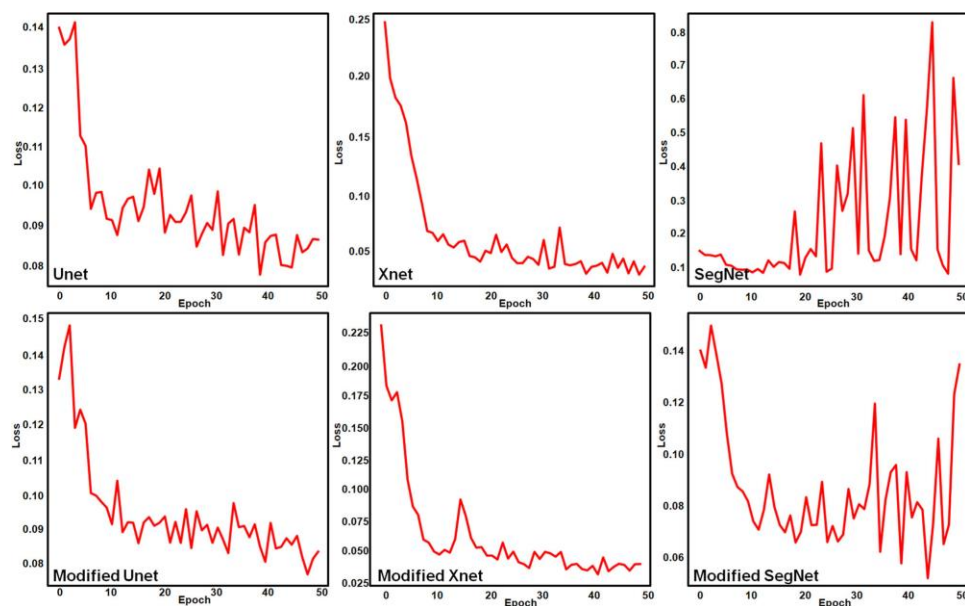


Figure 10

Figure 11 shows the behavior of the DL architectures for extracting regions with rice nutrient deficiency disorders. [Table 4](#) shows the quantitative results of extracting deficiency disorder regions. It was found that although the optimal loss for SegNet and Dilated U-EfficientNet after 50 epochs was found

to be between 0.2 and 0.4, frequent fluctuations were observed. Hence, these models were ignored along with the modified SegNet. The values of the loss function at each epoch showed that all the models except XNet and modified XNet suffered from very high overfitting. This overfitting got reduced to a large extent in XNet and modified XNet.

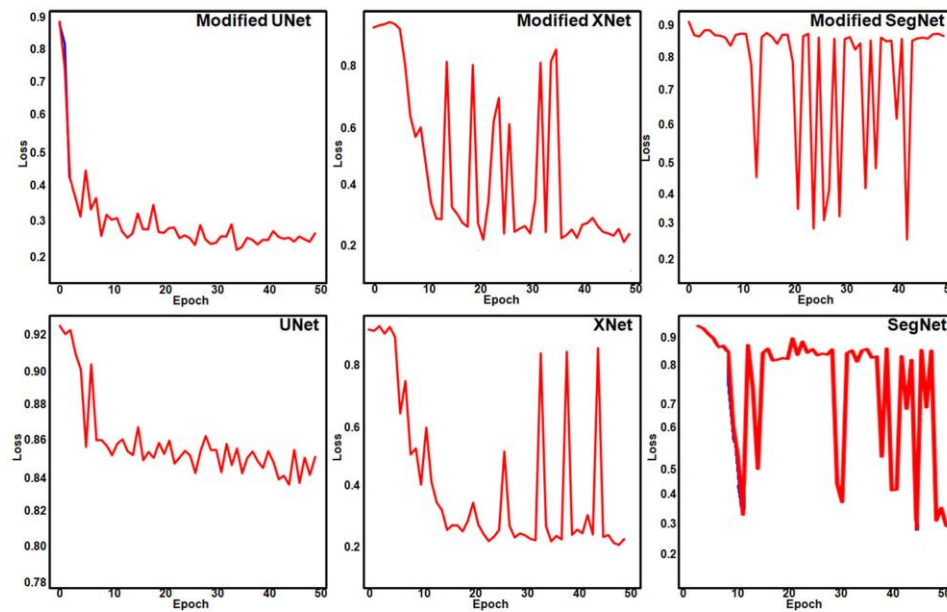


Figure 11

Validation loss curves during the extraction of rice deficiency disorder regions using DL segmentation.

Table 4

Quantitative results of extracting rice deficiency disorder regions using DL segmentation (module 1)

Models	Dice loss	Dice coefficient	Precision	Recall
UNet	0.0866	0.9134	0.9702	0.9673
XNet	0.0373	0.9627	0.9587	0.9717
SegNet	0.4034	0.5966	0.9913	0.4535
Modified UNet	0.0820	0.9180	0.9747	0.9697
Modified XNet	0.0363	0.9638	0.9490	0.9829
Modified SegNet	0.8636	0.1364	0.0769	0.7905

The average loss in the latter was decreased by 0.0004, which was considered the best model of the six DL models. The optimal loss value of the modified

XNet segmentation model changed from 0.2310 to 0.0362 throughout 50 epochs.

The qualitative results for the DL segmentation of infected rice leaves (disease and deficiency disorders) in the rice-infected region extraction module of the DeepBatch framework are shown in [Figure 12](#), where the white/yellow color indicates an infected region. In contrast, the black/purple color indicates a non-infected region. According to qualitative evaluation, a relative similarity is observed between the regions labeled by humans and those inferred by the best DL segmentation architecture. The refined segment obtained by applying bitwise logical AND operation on the images and their predicted masks is given attention in the next stage of DeepBatch. Finally, the predicted masks of rice diseases produced by dilated U-EfficientNet were considered as they showed the best performance. The predicted masks along with their respective RGB images underwent bitwise AND operation. In comparison with the human annotations, the ability of the best DL segmentation architecture to separate background pixels within infected regions is shown by the dice coefficient curves.

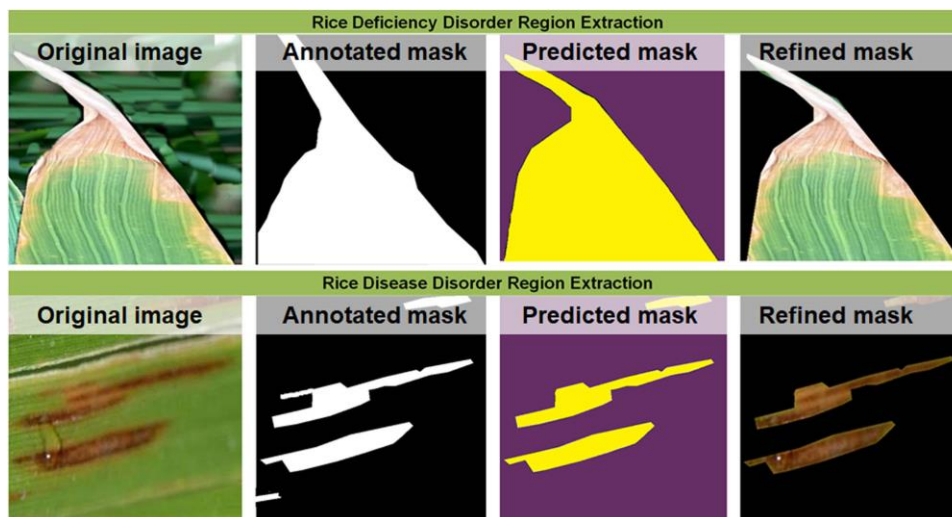


Figure 12

5 Conclusion

The DeepBatch methodology proposed in the current study makes use of DL-based segmentation and DL-based classification frameworks. The DL segmentation framework receives pre-processed images of the rice disease together with the corresponding masks. In order to predict the masks of the infected rice parts, the DL segmentation framework used modified versions of UNet, XNet, and SegNet. Bitwise multiplication was used to extract only the contaminated segment, leaving out the background and healthy sections. The DL classification framework receives these improved segmented images as inputs. For identifying diseases in rice plants, the second framework included both ensemble and TL architectures, which were carried out using five TL architectures: InceptionResNetV2, VGG19, Xception, DenseNet201, and MobileNet. The use of Xception, DenseNet201, InceptionResNetV2, and VGG19 produced 11 ensemble models. When compared to individual TL models, the ensembled models' performance was significantly better. Overall, it is observed that after applying the DeepBatch approach, the average accuracy of the TL models increased in both rice diseases and deficiency disorder images. The experiment demonstrates how the combination of various DL frameworks may be useful to design a rice disease/deficiency disorder diagnostic system. Future studies may concentrate on identifying disease and nutrient deficiency disorders in rice from a larger study region